

# PIV measurements of velocity of water in the presence of ice and comparison with calculated values

Christopher D. Seybert, James W. Evans \*

*Department of Materials Science and Engineering, University of California, 210 Hearst Mining Building, MC 1760, Berkeley, CA 94720, USA*

Received 17 July 2003; received in revised form 28 June 2004

## Abstract

Particle imaging velocimetry (PIV) has been used to measure the laminar natural convection resulting from buoyancy attendant on the freezing of water in a small rectangular cavity with transparent walls. The measured velocities show the “unusual” flow resulting from water having a density maximum at 277K. The PIV images also permitted the accurate determination of the shape and position of the solidification front in these quasi-steady experiments. The CFD software FLUENT® was used to simulate the flow and the position/shape of the solidification front with satisfactory results.

© 2004 Elsevier Ltd. All rights reserved.

## 1. Introduction and previous investigations

In many cases the important properties of materials are dependent on the microstructure established during solidification. Even when that microstructure is modified by subsequent processing (e.g. annealing) the final microstructure is dependent on the initial, post-solidification microstructure. Consequently solidification has been an ongoing topic of research for decades; texts [1,2] and conference proceedings [3,4] on the subject abound. One important aspect of solidification is the natural convection, driven by thermal or concentration gradients, that accompanies solidification in many instances. This flow transports heat and solute and causes other phenomena, such as the detachment of dendrite arms and the convection of the fragments, that play a

role in establishing solid microstructure [5]. What is reported on here are measurements and calculated results concerning the freezing of water where the natural convection that occurs displays an unusual feature. The objectives of the investigation were measurement of the unusual convection, to provide results for use by ourselves and other modelers, and the testing of software (FLUENT®) that has been used by us for modeling of natural convection associated with solidification (including natural convection in a magnetic field [6]).

Natural convection in cavities has been extensively worked on, however, the temperature–density relationship of the fluids in the investigations have typically been linear (or approximately so). Water, however, exhibits a density maximum at a temperature of 277K, and thus the fluid flow, heat transfer, and solidification process is altered when working in this temperature region. There are several other important fluids that exhibit density maximums, including gallium, bismuth, tellurium, and antimony. The relative ease of experimenting with

\* Corresponding author. Tel.: +1 510 642 3807; fax: +1 510 642 9164.

E-mail address: [evans@socrates.berkeley.edu](mailto:evans@socrates.berkeley.edu) (J.W. Evans).

the solidification of water might thus lend understanding in the solidification of these other materials.

Many other investigators have explored the peculiarities of flow around water's density extremum, although literature searches reveal no published results where velocities have been quantified (by methods such as particle image velocimetry) and compared to calculated results, as presented here. Joshi and Gebhart [7] measured the heat transfer characteristics and qualitatively visualized the fluid flow in transient and steady-state vertical natural convection. Braga and Viskanta [8,9] performed experiments on the transient cooling and solidification of water, visualizing the flow and collecting temperature data at various points within the rectangular cavity, comparing their results to numerical solutions. Other relevant investigations include those of Tankin and Farhadieh [10], Gebhart and Mollendorf [11], Brewster and Gebhart [12], and Ivey and Tankin [13].

## 2. Experimental apparatus and procedure

The measurements were carried out in the "cell" depicted in Fig. 1. The cell was designed to establish a controlled temperature gradient in one horizontal direction within a liquid confined between surfaces that were mostly transparent. One hollow copper block at each end served to control that gradient. Circulating inside the copper blocks was a mixture of ethylene glycol and water, held at constant temperature (within 0.05K) through the use of circulating water baths. The temperatures near the surfaces of the blocks adjacent to the liquid were monitored by thermocouples, which were inserted into small holes drilled into the blocks. Two different sizes of rectangular glass tubing were secured between the copper blocks. A 50mm long  $\times$  16mm  $\times$  16mm tube contained the liquid (distilled water in the present instance). A larger glass tube, 50mm long  $\times$

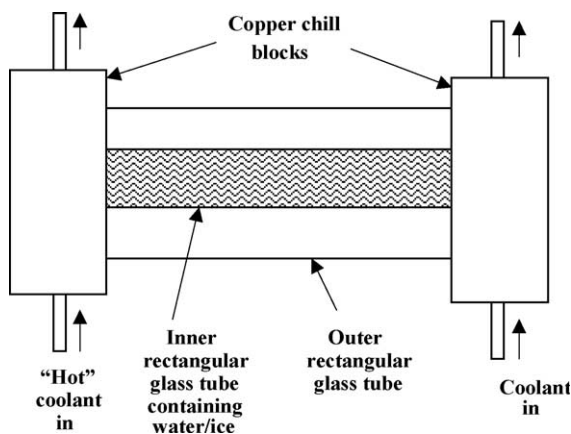


Fig. 1. Schematic of the experimental test cell.

35mm wide  $\times$  75mm tall, surrounded the smaller tube and served to provide some insulation between the liquid and the environment, and eliminate condensation on the surface of the smaller tube. The space between the tube was occupied by air.

The measurements were of velocity in the water and the position of the solidification front under quasi-steady state conditions (where the solidification front was stationary). This condition was achieved several tens of minutes after the coolant flows were started. Velocity measurements were carried out using particle image velocimetry (PIV). The water was seeded with hollow-glass spheres of a 15  $\mu$ m mean diameter. A thin sheet of light, approximately 0.5mm thick, was produced with a 30mW He-Ne laser and a cylindrical lens. The light sheet illuminated a vertical plane of the fluid, making visible the seed particles. The movement of the particles was recorded with a Pulnix TM-9701 CCD camera (768  $\times$  484 pixels) and EPIX framegrabber. This imaging system was capable of capturing 30 frames per second. The camera was placed with its optical axis horizontal and perpendicular to the light sheet. In this way, velocity components in the vertical direction and one horizontal direction could be measured. Image pairs were captured with precisely 15 frames separation (0.5s apart), as this was determined through experimentation to be optimal for the flow in this experiment. The imaged areas were 60mm  $\times$  36mm (high). Images were analyzed using a commercial software package, VidPIV<sup>®</sup>, developed by Optical Flow Systems Ltd. The interpolation area was 3 pixels by 3 pixels. In the experiments, velocities from 40 pairs of images were averaged together for the measurements. Although this is not necessary for laminar flows, it was found that the resultant plots were of better quality, the effects of random measurement errors being minimized. The solidification front was clearly discernible in the images and was plotted on the vector plots.

Preliminary experimental measurements in stagnant water gave settling velocities of approximately 8  $\mu$ m/s for the particles. Initially measurements with both copper blocks above the freezing point of water revealed the anticipated circulation (across the top of the cell from hot end to cold end and in the opposite direction across the bottom of the cell); the results of those measurements are in the thesis on which this paper is based [14].

## 3. Experimental results

Experimental results for the cold face of the cell at 268K and the "hot" face at 283K are given in Fig. 2. The irregular line passing downwards, towards the right of the plot, is the solidification front. Speeds range up to approximately 0.5mm/s. At first the results appear unremarkable. Warmer water is rising at the hot surface on

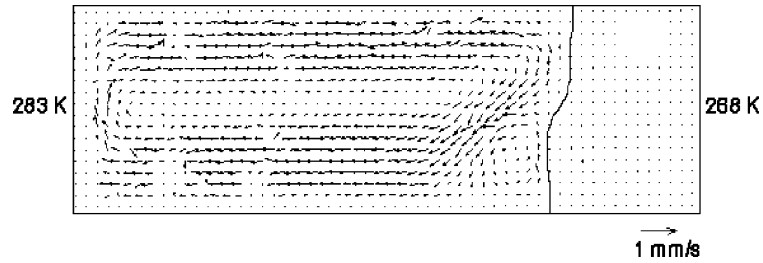


Fig. 2. Steady state PIV vector plot of water. The hot side has been held at 283 K; cold side is at 268 K.

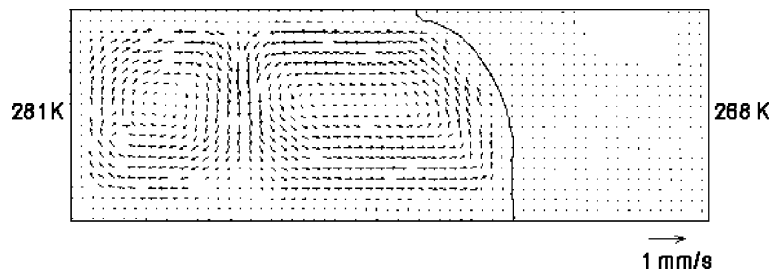


Fig. 3. PIV vector plot of water at a steady state of solidification. The hot side has been held at 281 K in this case. Flow can be seen to be upward on both the hot and cold sides.

the left, crossing the top of the cell in the anticipated direction and impacting the top of the solidification front (causing that front to be less advanced in its upper part). The flow then descends most of the solidification front before returning to the left. However, a small secondary circulation loop is clearly visible near the lower part of the solidification front. It is conjectured that this is due to the unusual variation, with temperature, of the density of water. The density of water *increases* between 273 K and 277 K and thereafter decreases as water expands in the normal way.

This conjecture is supported by the results of Fig. 3 (and also by computed results presented in the next section), where the temperature of the hot face is lower (281 K) than in Fig. 2. The flow upward along the hot face, driven by the buoyancy of the normal expansion of a liquid, is matched by a counter flow upward at the solidification front, driven by buoyancy resulting

from the unusual expansion of the water as it cools near its freezing point. The shape of the circulation front is different from that in Fig. 2. The impacting flow is now at the bottom of the ice and it is therefore here that the front is less advanced.

The final set of experimental results presented here are in Fig. 4. Now the hot face is at 278 K, i.e. just above the temperature for the density maximum. The flow is now dominated by the convection arising from the unusual density gradient.

#### 4. CFD calculations of the flow, temperatures and solidification front

Mathematical modeling of the experiment was accomplished using the commercial CFD software package FLUENT®. After the input of relevant properties

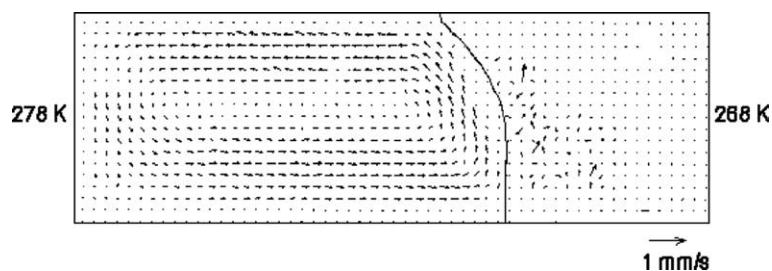


Fig. 4. Steady-state PIV vector plot of water solidification where the hot side is at 278 K and the cold side is at 268 K.

and boundary conditions and the selection of various solution methods and parameters (i.e. under-relaxation factors and discretization schemes), FLUENT solves the coupled continuity, energy, and Navier–Stokes equations. As these simulations were modeling natural convection, the force of gravity was included in the Navier–Stokes equations with a temperature dependent density term. Laminar flow was assumed. The no-slip condition was imposed at the liquid boundaries. Temperatures were specified at the water/copper block and ice/copper block interfaces. Heat fluxes at the interfaces with the glass walls, top and bottom were set to zero.

The contents of the cell were treated as one continuum with the viscosity increased to a high value (2 kg/ms) at the points where the water lay below the freezing point. This high value was sufficient to render velocities in the ice negligible. The 16 mm × 16 mm × 50 mm water volume was simulated with nodes at 0.2 mm intervals, selected after preliminary calculations to check for mesh sensitivity. Both 3D and 2D calculations were performed, the latter in the center plane corresponding to the plane of the experimental measurements. Negligible differences in velocity were found between 3D and 2D results at this plane in preliminary calculations [15]. Consequently the results presented below are for 2D calculations. The segregated implicit solver was used in all calculations. The interpolation scheme chosen was the Quadratic Upwind (QUICK) scheme. This is appropri-

ate because of the uniform quadratic mesh used, and provides third order accuracy. A comparison with first-order and second-order upwind schemes appears in Seybert [14].

The equation for the density of water (valid from 273 K to 290 K) was derived from literature data [15] and was (kg/m<sup>3</sup>).

$$\rho = 456.490 + 3.925T - .007085T^2$$

The density of ice was set to its value at the freezing point as thermal contraction of the ice was assumed negligible over the small temperature range (5 K).

Viscosity was entered as a piecewise polynomial equation. Below 273 K the viscosity was set to 2 kg/ms to simulate a solid and above 273 K the viscosity was:

$$\mu = 0.08771 - 5.724 \times 10^{-4}T + 9.437 \times 10^{-7}T^2$$

as derived from literature values [15], where  $\mu$  is the viscosity in kg/ms. Thermal conductivity was entered as a constant 0.6 W/m K above 273 K, and 2.09 W/m K below 273 K. The specific heat of water was assumed a constant 4152 J/kg K. As the simulations were for the quasi-steady state (no advancement/retraction of the solidification front) the latent heat of solidification was not required.

Fig. 5 displays the computed velocity vectors and isotherms for the cell cold face at 268 K and the hot face at 283 K and is to be compared with the experimental re-

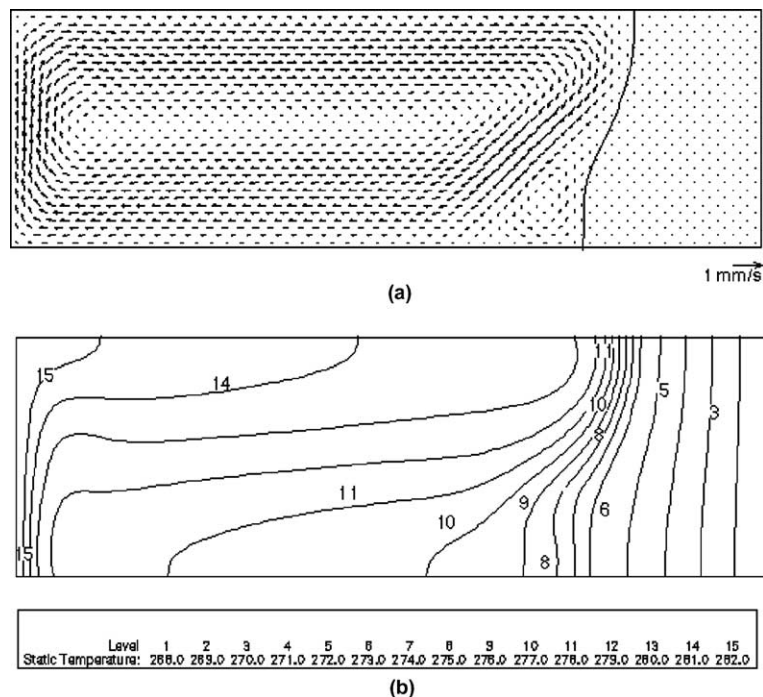


Fig. 5. Model results for the solidification of water, hot wall held at 283 K, cold wall at 268 K: (a) vector plot, (b) temperature contours.

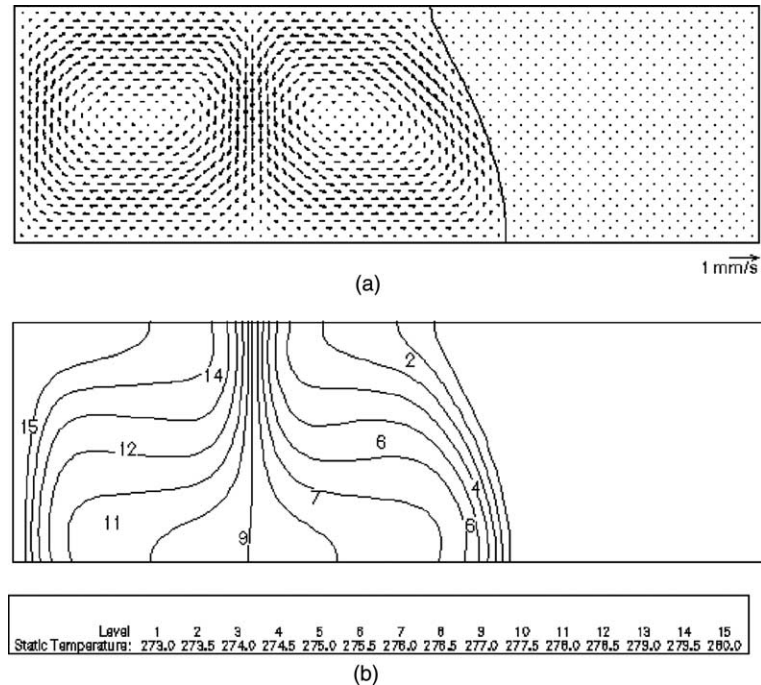


Fig. 6. Model results for the solidification of water, hot wall held at 281 K, cold wall at 268 K: (a) vector plot, (b) temperature contours.

sults of Fig. 2. It is seen that FLUENT® is able to capture the general pattern of the flow: a clockwise recirculation in the bulk of the liquid volume with a smaller counterclockwise recirculation near the bottom of the solidification front. The shape and position of the calculated solidification front are also similar to the measured ones. The Fig. 5(b) contains the computed isotherms; the one closest to the temperature of maximum density is that labeled 10 and it lies near the center of the stream of water descending near the solidification front.

Fig. 6 shows the computed velocities, solidification front and isotherms for the case corresponding to Fig. 3 with the cold face at 268 K and the hot face at 281 K. Again the computed flow pattern and that discernible in the experimental measurements agree. There is the downflow in the middle of the liquid volume corresponding to the density maximum (near isotherm 9 in Fig. 6(b)) with a normal natural convection to the left and the unusual convection to the right. Note that the shape of the solidification front is different in Fig. 6 from that in Fig. 5 in the same way that the shape in Fig. 3 is different from that in Fig. 2. A more direct comparison of computed and measured velocities is presented in Fig. 7 where the horizontal velocity is plotted versus position along a horizontal line near the top of the cell. The computed and measured velocities agree well but for a displacement in position of a few mm perhaps resulting from that difference in the location of the solidification front.

In Fig. 8 the computed results for the cold face at 268 K and the hot face at 278 K are shown and should be compared to the experimental results in Fig. 4. The results for circulation pattern, velocity and solidification front appear to be in reasonable agreement.

Finally, in Fig. 9 the measured and computed positions of the solidification front (top and bottom of the water) are plotted versus the hot side temperature. There

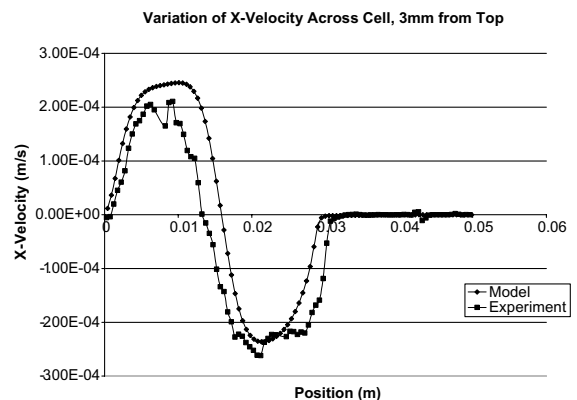


Fig. 7. Values of  $x$ -velocity across the cell are compared for the model and experiment. The data were taken from 3 mm below the top of the cell, from hot side to cold side, and are for the 8°C case.

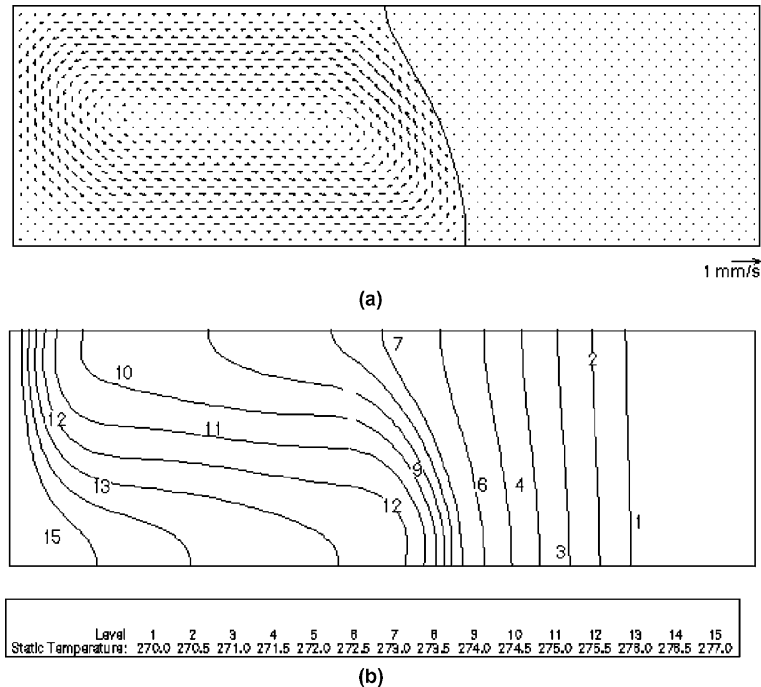


Fig. 8. Model results for the solidification of water, hot wall held at 278 K, cold wall at 268 K: (a) vector plot, (b) temperature contours.

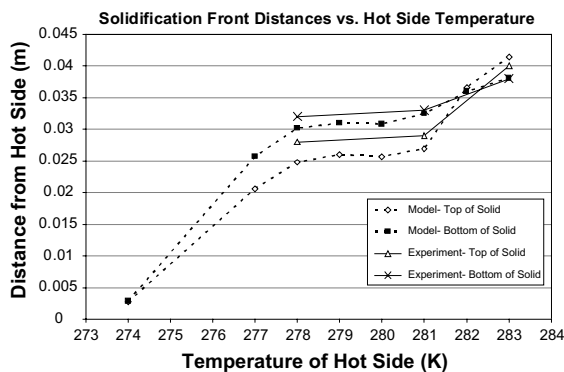


Fig. 9. The distance of the solidification front from the hot side for various hot side temperatures.

is agreement to within a few mms. and the hot side temperature at which the top of the ice advances beyond the bottom are within 1 K of 282 K for both experimental and computed results.

## 5. Discussion

The measured velocities of the order of 1 mm/s yield a Reynolds number of approximately 1.6 (defined in the usual way using the cell height as the characteristic

dimension) and a Peclet number of 350 (cell length). The former is some justification for the assumption of laminar flow in the FLUENT® calculations. The large Peclet number is consistent with the influence of the water circulation pattern on the measured and computed solidification front shape, as well as on the isotherms displayed in the lower halves of Figs. 5, 6 and 8.

This investigation shows that there is reasonable agreement between measurements and computed velocities resulting from use of FLUENT®. The simulations are also successful in simulating the positions of the solidification front at steady state, as well as showing the unusual circulation pattern, due to the density extremum, seen in the PIV results.

It is appropriate to consider whether this agreement would hold for the dynamic conditions of advancement or retraction of the ice–water interface. The measured and calculated velocities were quasi-steady ones and agreement might be poorer when accelerations result from changes in liquid volume. However, even in the case of an advancing (or retreating) interface, transport of momentum and heat in the liquid is likely to be at quasi-steady state. With only diffusive momentum transport, the relaxation time for establishment of steady velocities in the liquid is of order one minute versus several tens of minutes for freezing of the whole volume of the cell. The time for convective heat transport is also of the order of 1 min. However the relaxation time for

establishment of steady temperatures by conduction in 25mm of ice is of the order of 20min. Consequently the success of FLUENT® in simulating the dynamics of freezing hinges on its ability to represent unsteady heat transport in the ice, which appears to be a simple task and one might expect agreement in the dynamic case where the solidification front is not stationary. There are of course fewer grounds for optimism when the scale of the system/velocities are larger and the flow becomes turbulent.

## 6. Concluding remarks

In this investigation PIV has been used to measure the velocities of water in a cell containing partially frozen water. Flow was driven by density gradients resulting from temperature gradients and the unusual temperature dependence of the density of water, near 277 K, was found to have a significant effect on the flow. The measurements of velocity match computed velocities obtained from the commercial CFD code FLUENT®. Furthermore the shape and position of the solidification front predicted by FLUENT® are also in agreement with the measurements.

## Acknowledgment

Research supported by NASA under grant 96-HEDS-02-063.

## References

- [1] M.C. Flemings, *Solidification Processing*, McGraw-Hill, New York, 1974.
- [2] W. Kurtz, D.J. Fischer, *Fundamentals of Solidification*, Trans Tech Publications, Aedermannsdorf, Switzerland, 1992.
- [3] B.G. Thomas, C. Beckermann (Eds.), *Modeling of Casting, Welding and Advanced Solidification Processes—VIII*, TMS, Warrendale, PA, 1998.
- [4] Special Issue on Recent Advances in Solidification, *ISIJ International*, vol. 35(6), 1995.
- [5] C.J. Paradies, M.E. Glicksman, R.N. Smith, The influence of forced convection during solidification on fragmentation of the mushy zone of a model alloy, in: J.W. Evans (Ed.), *Light Metals*, TMS, Warrendale, PA, 1995.
- [6] C.D. Seybert, J.W. Evans, F. Leslie, W.K. Jones Jr., Suppression/reversal of natural convection by exploiting the temperature/composition dependence of magnetic susceptibility, *J. Appl. Phys.* 88 (7) (2000) 4347–4351.
- [7] Y. Joshi, B. Gebhart, Measurements and visualizations of transient and steady-state vertical natural convection flow in cold water, *Int. J. Heat Mass Transfer* 29 (11) (1986) 1723–1740.
- [8] S.L. Braga, R. Viskanta, Transient natural convection of water near its density extremum in a rectangular cavity, *Int. J. Heat Mass Transfer* 35 (1992) 861–875.
- [9] S.L. Braga, R. Viskanta, Effect of density extremum on the solidification of water on a vertical wall of a rectangular cavity, *Experimental Thermal and Fluid Science* 5 (1992) 703–713.
- [10] R.S. Tankin, R. Farhadieh, Effects of thermal convection currents on formation of ice, *Int. J. Heat Mass Transfer* 14 (1971) 953–961.
- [11] B. Gebhart, J.C. Mollendorf, Bouyancy-induced flows in water under conditions in which density extrema may arise, *J. Fluid Mech.* 89 (1978) 673–707.
- [12] R.A. Brewster, B. Gebhart, An experimental-study of natural-convection effects on downward freezing of pure water, *Int. J. Heat Mass Transfer* 31 (2) (1988) 331–348.
- [13] G.N. Ivey, P.F. Hamblin, Convection near the temperature of maximum density for high Rayleigh number, *J. Heat Transfer—Transactions of the ASME* 111 (1) (1989) 100–105.
- [14] C.D. Seybert, Exploiting magnetic susceptibility variations to control convection, M.S. thesis, University of California, Berkeley, 2000.
- [15] R.C. Weast (Ed.), *Handbook of Chemistry and Physics*, seventieth ed., CRC Press, Boca Raton, FL, 1989.